

CONFRONTING THE JET MODEL OF SGR A* WITH THE FARADAY ROTATION MEASURE OBSERVATIONS

YA-PING LI¹, FENG YUAN^{2,1}, Q. DANIEL WANG³¹Department of Astronomy and Institute of Theoretical Physics and Astrophysics, Xiamen University, Xiamen, Fujian 361005, China
²Shanghai Astronomical Observatory, Chinese Academy of Sciences, 80 Nandan Road, Shanghai 200030, China, fyuan@shao.ac.cn and
³Department of Astronomy, University of Massachusetts, Amherst, MA 01003, USA, wqd@astro.umass.edu*Draft version March 21, 2021*

ABSTRACT

Sgr A* is probably the supermassive black hole being investigated most extensively due to its proximity. Several theoretical models for its steady state emission have been proposed in the past two decades. Both the radiative-inefficient accretion flow and the jet model have been shown to well explain the observed spectral energy distribution. Faraday rotation measure (RM) has been unambiguously measured at submillimeter wavelength, but has only been tested against the accretion flow model. Here we first calculate the RM based on the jet model and find that the predicted value is two orders of magnitude lower than the measured value. We then include an additional contribution from the accretion flow in front of the jet and show that the measured RM may be reconciled with the model under some tight constraints. The main constraint is that the inclination angle should be greater than $\sim 73^\circ$. But this requirement is not consistent with an existing observational estimate of the inclination angle.

Subject headings: Galaxy: center—ISM: jets and outflows—black hole physics—accretion, accretion disks

1. INTRODUCTION

Because of its proximity, Sgr A* at the center of our Galaxy presents us as a unique laboratory to study the low-luminosity accretion process of supermassive black holes (SMBHs; see Genzel, Eisenhauer & Gillessen 2010; Falcke & Markoff 2013; and Yuan & Narayan 2014 for the most recent reviews focusing on different aspects of Sgr A*). With a mass of $4 \times 10^6 M_\odot$ (Schödel et al. 2002; Ghez et al. 2008; Gillessen et al. 2009; Meyer et al. 2012), Sgr A* has a bolometric luminosity of only $10^{36} \text{ erg s}^{-1} \approx 3 \times 10^{-9} L_{\text{Edd}}$, the bulk of which is emitted in the submillimeter bump. High spatial resolution *Chandra* observations have resolved the Bondi radius, $R_{\text{Bondi}} \approx 4'' (\approx 4 \times 10^5 R_S)$, where $R_S \equiv 2GM_{\text{BH}}/c^2$ is the Schwarzschild radius of Sgr A* given that the temperature of the ambient plasma as 1 keV (Baganoff et al. 2003, Wang et al. 2013). In combination with the inferred gas density at the Bondi radius as $\simeq 100 \text{ cm}^{-3}$ (Baganoff et al. 2003), the Bondi accretion rate is estimated to be $\dot{M}_B \approx 10^{-5} M_\odot \text{ yr}^{-1}$, which is in good agreement with the three-dimensional numerical simulation for the accretion of stellar winds onto Sgr A* by Cuadra et al. (2006). The low luminosity combined with the Bondi accretion rate indicates that the radiative efficiency of Sgr A* is extremely low, $\eta \approx 10^{-6}$.

In addition to the continuum spectrum, a high level of linear polarization (2% \sim 10%) at frequencies higher than $\sim 150 \text{ GHz}$ has been detected (Aitken et al. 2000; Bower et al. 2005; Macquart et al. 2006). This detection provides us with a tool to measure the magnetized plasma through the Faraday rotation of the polarized light. The rotation of the polarization angle is expressed as $\chi = \chi_0 + \text{RM}\lambda^2$ (where χ_0 is the intrinsic polarization angle, while λ is the observed wavelength). The observed rotation measure (RM) of Sgr A* can thus serve as a probe of the electron density weighted by the line of sight components of the magnetic field toward these

central engines¹. Obviously, any acceptable theoretical models must satisfy both the continuum spectrum and polarization observations.

Marrone et al. (2007) made the first reliable determination of the RM for Sgr A* with simultaneous observations at multiple frequencies, using the Submillimeter Array (SMA) polarimeter; the mean RM is $-5.6 \pm 0.7 \times 10^5 \text{ rad m}^{-2}$ while a conservative 3σ upper limit to the variation of the RM is $2 \times 10^5 \text{ rad m}^{-2}$ (Marrone et al. 2007). This unambiguous detection of the RM limits the accretion rate close to the black hole to be in the range of $(2 \times 10^{-7} - 2 \times 10^{-9}) M_\odot \text{ yr}^{-1}$, depending on the configuration of the magnetic field.

Accompanied by the observational progresses, numerous theoretical efforts on modelling the quiescent state emission of Sgr A* have been made, including the development of the radiatively inefficient accretion flow (RIAF) model (Yuan, Quataert & Narayan 2003; see Yuan & Narayan 2014 for the most recent review on RIAF theory and its applications), jet model (e.g., Falcke & Markoff 2000, see also for the updated jet model by Markoff et al. 2007 and Mościbrodzka & Falcke 2013), jet-advection dominated accretion flow (ADAF) model (Yuan et al. 2002) and spherical accretion model (e.g., Melia 1992; Melia, Liu & Coker 2000).

In particular, both the jet and RIAF models have successfully explained the spectrum (Falcke & Markoff 2000; Yuan, Quataert & Narayan 2003) and the size of Sgr A* (Falcke & Markoff 2000; Yuan et al. 2006; Huang et al. 2007; Markoff et al. 2007, see Doeleman et al. (2008) for

¹ The first RM towards the extragalactic radio source was made by Cooper & Price (1962). Since then many VLBI observations (e.g., Udomprasert et al. 1997; Taylor 1998, 2000; Asada et al. 2002; Zavala & Taylor 2002, 2003; Gabuzda et al. 2004) have been carried out to reveal the parsec-scale (i.e., jet) RM properties for quasars, radio galaxies, and BL Lac objects. The time variabilities and distributions of the observed RMs suggest that they are primarily intrinsic to active galactic nuclei (AGNs).

the current inferred size from 1.3 mm VLBI observations). The two models are difficult to distinguish in this sense. The RIAF model has also explained the polarization and RM. The “old” version of the RIAF model (i.e., the classical ADAF without outflow, see Narayan et al. 1995; Manmoto et al. 1997; Narayan et al. 1998) *assumes* that the accretion rate is independent of radius. This leads to a large electron number density in the inner region of the accretion flow and thus a large RM, which significantly depolarizes the polarized emission. Interestingly, before the detection of the radio polarization in Sgr A*, theoretical works had begun to show that very little mass available at large radii could actually accrete into the inner most region around the SMBH (e.g., Stone, Pringle & Begelman 1999; Hawley & Balbus 2002; Igumenshchev, Narayan & Abramowicz 2003; see Yuan, Wu & Bu 2012 for a review). This development could then solve the polarization problem, as explained in the updated RIAF model presented in Yuan, Quataert & Narayan (2003). The inward decrease of mass accretion rate was explained either due to outflow (ADIOS; e.g., Blandford & Begelman 1999; Begelman 2012) or to convection (e.g., Narayan et al. 2000; Quataert & Gruzinov 2000a). Yuan, Bu & Wu (2012; see also Narayan et al. 2012 and Li, Ostriker & Sunyaev 2013) has shown that outflow rather than convection is responsible for the inward decrease of the accretion rate. Such a theoretical prediction has been confirmed by the 3M second *Chandra* observations of Sgr A* (Wang et al. 2013).

In this work, we calculate the RM for the jet model. Our calculations give RM far below the observed value mentioned above (Marrone et al. 2007). Along the line of sight (LOS) toward the jet “nozzle”, the accretion flow should also contribute to the observed RM. This contribution depends on the viewing path through the structure of the accretion flow. We can thus either rule out the jet model or set a tight constraint on the viewing geometry.

In the rest of the paper, we present our RM calculations based on the jet model in Section 2 and calculate the RM contribution from the accretion flow in Section 3. Discussions on the implications of the results are given in Section 4. We summarize our results and conclusions in Section 5. Throughout this work, we assume the SMBH mass as $4 \times 10^6 M_\odot$ for Sgr A* and its distance to be 8 kpc.

2. JET MODEL AND ITS ROTATION MEASURE

We follow the jet model presented in Falcke & Markoff 2000 (hereafter FM00, namely the “old” jet model). In this model the submillimeter emission of Sgr A* comes from the acceleration region of the jet close to the black hole, called “nozzle”. The sharp spectral cut-off on the infrared (IR) side of the submillimeter bump requires a narrow electron energy distribution in the nozzle. Thus two cases are considered, namely 1) a power-law electron energy distribution with the index $q = 2$ and with a steep cut-off at $5\gamma_{e,0}$ and 2) a relativistic Maxwellian distribution with $\gamma_{e,0} \approx \frac{kT}{m_e c^2}$. The “free” parameters in the nozzle component such as the magnetic field B_0 , the electron Lorentz factor $\gamma_{e,0}$, the total electron density n_0 , and the nozzle length scale z_0 (sonic point) are constrained

by the submillimeter spectrum. Beyond the jet nozzle, the magnetized, relativistic plasma is ejected from the nozzle to form the extended jet, where the plasma is accelerated along the jet axis through the pressure gradient and expands sideways with its initial sound speed in units of the speed of light, $\beta_{s,0} = \sqrt{\Gamma(\Gamma-1)/(\Gamma+1)}$ (where $\Gamma = 4/3$ is the adiabatic index). The velocity field β_j in the extended jet with the bulk Lorentz factor γ_j follows the modified, relativistic Euler equation. Algebraic transformations then lead to

$$\frac{\partial \gamma_j \beta_j}{\partial z} \left(\frac{\left(\frac{\Gamma+\xi}{\Gamma-1} \right) (\gamma_j \beta_j)^2 - \Gamma}{\gamma_j \beta_j} \right) = \frac{2}{z} \quad (1)$$

with $\xi = (\gamma_j \beta_j / (\Gamma(\Gamma-1)/(\Gamma+1)))^{1-\Gamma}$.

The equation can be solved with the critical point condition $\beta_j = \beta_{s,0}$ at $z = z_0$. Taking adiabatic cooling due to the longitudinal pressure gradient and lateral expansion (FM00) into account, one can also determine the evolution profiles of the electron number density $n(z)$, magnetic field $B(z)$ and electron Lorentz factor $\gamma_e(z)$ along the z axis in a cylindrical coordinate system, which are shown in Fig. 1.

The total jet synchrotron emission can be obtained by integrating along the z axis. As we only care about the submillimeter emission, SSC process which only contributes to the high energy band (here X-ray) is neglected in the following calculation. The modification due to general relativistic effects on the spectrum is not included. Due to the Doppler boosting effect, we only consider the emission from the approaching jet. The fitting spectrum with the nozzle parameters is shown in Fig 3. The parameters we adopt to fit the spectrum are quite similar to those in FM00 (see also Markoff et al. 2007), with only slight adjustments due to the different mass and distance of the SMBH adopted here. Specifically, the inclination angle θ_i is determined in the spectral modelling via the Doppler boosting factor. Note that the difference of $\gamma_{e,0}$ for the Maxwellian electron energy distribution with FM00 is only because of the different definition of $\gamma_{e,0}$.

We then calculate the RM in the nozzle region along our LOS as

$$\text{RM} = 8.1 \times 10^5 \int \frac{\log \gamma_e(z)}{2\gamma_e^2(z)} n_e(z) \mathbf{B} \cdot d\mathbf{l} \text{ rad m}^{-2} \quad (2)$$

for the electron density n_e in units of cm^{-3} , the path length $d\mathbf{l}$ in units of pc, and the magnetic field \mathbf{B} in units of Gauss. The factor $\log \gamma_e(z)/2\gamma_e^2(z)$ is due to the relativistic correction (Quataert & Gruzinov 2000b). In the thermal case, the electron temperature T is related to the Lorentz factor γ_e by $\gamma_e = kT/m_e c^2$. The above equation should be applied to the external Faraday rotation, which means that the emitting region and Faraday rotator exist separately. For the case of internal Faraday rotation considered here, namely, both the emission and Faraday rotator are contributed by the jet, there is an additional correction factor of $\sim 1/2$ to the Eq. 2 (Burn 1966; Homan 2012)². Following the GRMHD numerical

² The correction factor for internal Faraday rotation depends on the physical and viewing geometry of the emission region. The

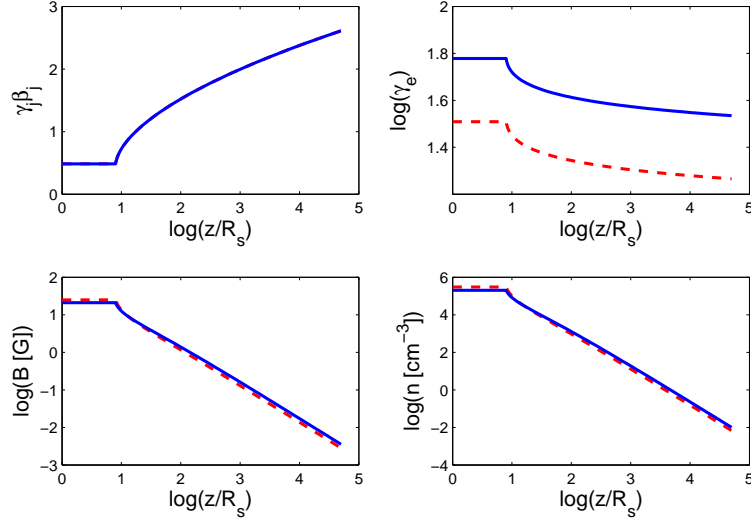


FIG. 1.— The jet dynamical profile of $\gamma_j\beta_j$, Lorentz factor γ_e , magnetic field B , and electron density n_e along the z -axis. The solid (dashed) line is for the case of the power-law (Maxwellian) distribution of electrons.

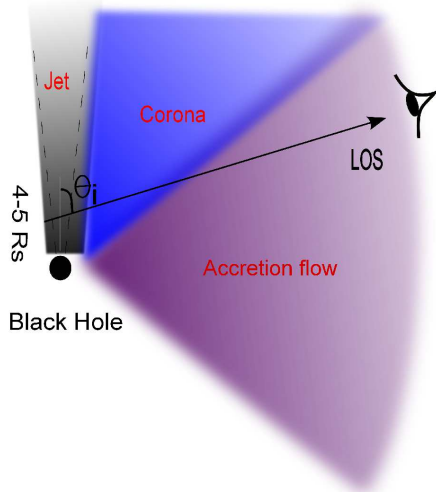


FIG. 2.— The cross-section structure of the jet and accretion flow (including the corona) of Sgr A* in the $r - \theta$ plane (refer to Fig. 4 in Yuan & Narayan (2014) for the more precise MHD numerical simulation result). The black thick solid line denotes one representative sight-line through the plane. The dashed line presents the radial geometry of the magnetic field.

simulations of the accretion flow and jet formation (see review by Yuan & Narayan 2014 and Fig. 4 of that paper), we find that the magnetic field in the jet is mainly radial and contains no reversals along our line of sight. The ordered magnetic field we adopt presents an upper limit of the RM considered here.

factor of $1/2$ is only true for an cylinder whose axis is parallel to the LOS and $\Delta\chi < 90^\circ$. For other case, this factor differs a little but is also around $1/2$ (Cioffi & Jones 1980).

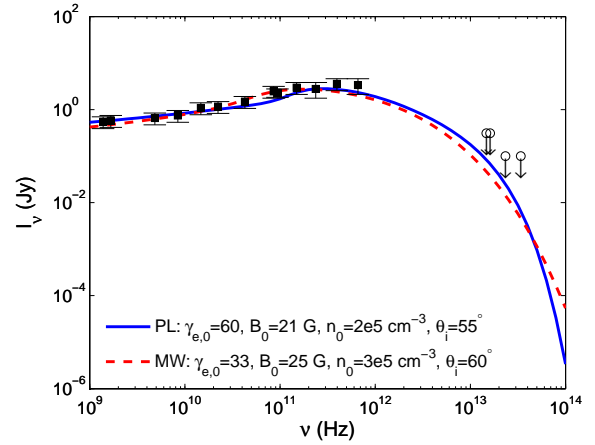


FIG. 3.— The fitting spectrum of Sgr A* with the observation data from FM00 (infrared data shown as open circle are all upper limit.). Although these data may not be the latest, we do not expect that any update would significantly affect our fitting and hence the following RM results. The solid blue line is for a power-law (PL) electron energy distribution with an index of $q = 2$ and the dashed red line for a relativistic Maxwellian distribution (MW) with $\gamma_e = kT/mec^2$. The radius of the jet nozzle $r_0 \simeq 2.4R_s$ and its height $z_0 = 8R_s$ are assumed.

In the case of thermal electrons, the integration of Eq. 2 for the thermal electrons in the nozzle region gives

$$\text{RM} \approx 7.7 \times 10^3 \text{ rad m}^{-2}, \quad (3)$$

which is two orders of magnitude less than the observed value (Marrone et al. 2007). In the case of power-law electrons, the result is similar, which is $\text{RM} \approx 1.2 \times 10^3 \text{ rad m}^{-2}$. The point of the integration begins from the far side of the jet surface at the $4-5R_s$ from the black hole (see Fig. 2) to the near side of the jet. This integration all the way down to the innermost region of the

jet nozzle neglects the optical depth effect on its RM. If the emitting plasma is optically thick, this calculation should be regarded as an upper limit, which means that the corresponding RM will be far below the observed value. We feel that there is little room to adjust the model parameters to increase the RM value to match the observed one. Compared to the RIAF model of Yuan, Quataert & Narayan (2003), the strength of the magnetic field is similar, the small value of the RM is mainly because of the electrons density in the nozzle being much lower than that in the accretion flow. The dramatic discrepancy between the jet and the observation for the RM thus puts a challenge to the jet model.

3. ACCRETION FLOW CONTRIBUTION TO THE RM

A possible contribution to the observed RM, in addition to the jet itself, may come from the accretion flow around Sgr A* (see the illustration shown in Fig. 2). The RM contribution from the accretion flow depends on the distributions of the electron density and magnetic field in the r - θ plane of the accretion flow. We obtain such information from the multidimensional MHD numerical simulations (De Villiers et al. 2005; Yuan, Wu & Bu 2012).

Based on a numerical simulation with the radial dynamical range as large as four orders of magnitude, Yuan, Wu & Bu (2012; see also references therein) show that the radial density profile of the accretion flow can be well described by a power-law form, namely $n_e \propto r^{-p}$, with the index p in the range of 0.5 – 1.0. The temperature profile is described by $T_e \propto r^{-1}$.

The strength of the magnetic field is tied to the density roughly by a parameter $\beta \equiv p_{\text{gas}}/(p_{\text{gas}} + p_{\text{mag}})$, where p_{gas} and p_{mag} are the gas and magnetic pressures). The value of β is typically ~ 0.9 (see review by Yuan & Narayan 2014). But for the “magnetically arrested disk” (“MAD”) (Narayan et al. 2003; Tchekhovskoy et al. 2011; Tchekhovskoy & McKinney 2012; Narayan et al. 2012; McKinney, Tchekhovskoy & Blandford 2012), the value of β can be smaller, i.e., the magnetic field is stronger. But even in this case, current MHD simulations indicate that the field energy can at most be in equipartition with the thermal energy, i.e., $\beta \gtrsim 0.5$. We therefore consider $0.5 \lesssim \beta \lesssim 0.9$. The configuration of the magnetic field is less well determined. The MHD numerical simulation can give us some suggestions, which, however, somewhat depend on the initial configuration of the field. Without losing generality, we can simply assume a radial configuration. In reality, this should be multiplied by a factor of “ $\cos(\alpha)$ ” to account for the effect of the inclination angle α of the magnetic field relative to our LOS. This would greatly reduce the RM contribution from the accretion flow. So our calculation for the case of pure radial magnetic field gives an upper limit to the RM contributed by the accretion flow, which we will see will not change our conclusion presented below. Furthermore, based on fully relativistic three-dimensional numerical simulations of accretion flows under the Kerr metric, De Villiers et al. (2005) find that the density and gas pressure decrease exponentially with polar angle (see Fig. 3 of that paper).

With the corresponding distributions normalized to the values at the Bondi radius as inferred from *Chandra* data (Baganoff et al. 2003; Wang et al. 2013), we ob-

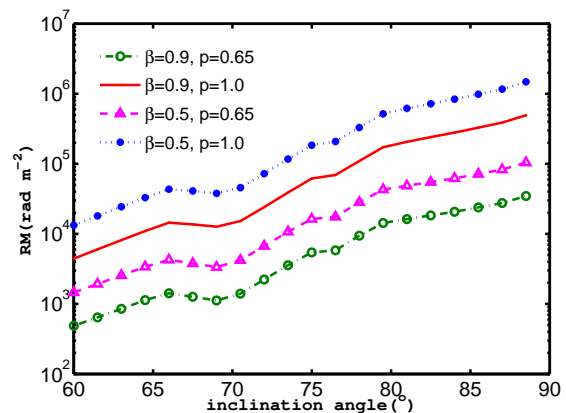


FIG. 4.— RM contribution from the accretion flow as a function of the viewing angle for four different model parameter sets (p , β). Only the red solid and blue dotted lines, which correspond to $p = 1.0$ and $\beta = 0.5 - 0.9$, can reach the magnitude of the observed RM, $\sim 10^5$ rad m $^{-2}$.

tain the density, temperature, and magnetic field at each point in the r - θ plane of the accretion flow. The integration of Eq. 2 along the line of sight then gives the corresponding RM as a function of the viewing angle for different parameters p and β . The jet inclination angle (θ_i) is also considered as a free parameter, although it has a preferred value (see later discussion). Fig. 4 shows that a smaller β (i.e., stronger magnetic field) and/or a larger p (i.e., weaker wind) can produce a larger RM. This is easy to understand. Only for the red solid and blue dotted lines, which correspond to $p = 1.0$ and $\beta = 0.5 - 0.9$, plus an inclination angle $\theta_i \gtrsim 73^\circ$, or equivalently the angle between our line of sight and the equatorial plane of the accretion flow $\lesssim 17^\circ$, can we obtain the magnitude of the observed RM, $\sim 10^5$ rad m $^{-2}$.

Whether the above values of p and β are reasonable? As stated above, the MHD numerical simulations of the hot accretion flow have shown that $\beta = 0.5 - 0.9$ is reasonable. The value of $p = 1$ is close to its upper limit obtained from numerical simulations and the modelling of Sgr A* (Yuan, Quataert & Narayan 2003), although it is larger than that obtained from fitting the iron lines, which is $p \sim 0.5$ (Wang et al. 2013). Given the model and measurement uncertainties, however, we can conclude that the above-mentioned “required” values of p and β are roughly consistent with the current theoretical and observational constraints. In this case, the main constraint will be on the inclination angle. The required large angle means that our LOS should intersect with the accretion disk close to its equatorial plane.

4. DISCUSSION

Is this inclination angle requirement consistent with the reality? First, there are a few model constraints on the orientation of the black hole spin. But all these constraints are based on the assumption that the observed submillimeter radiation of Sgr A* comes from the hot accretion flow rather than the jet, in either the analytical RIAF model (Yuan, Quataert & Narayan 2003; see also Huang et al. 2007; Broderick et al. 2011) or the MHD numerical simulations (e.g., Sharma et al.

2007; Mościbrodzka et al. 2009; Dexter et al. 2010; Shcherbakov et al. 2012). Thus such constraints do not apply here.

Second, it is widely accepted that accretion materials onto Sgr A* are mainly supplied by winds from circumnuclear massive stars (e.g., Cuadra et al. 2008). These stars are primarily in a disk, which has an inclination of $\theta_i \sim 53^\circ$ and a line-of-nodes position angle of $\sim 100^\circ$ (east from north, Paumard et al. (2006)). One may expect that the angular momentum of this stellar disk and its inclination are reflected in the accretion flow morphology projected in the sky. Indeed, this expectation has been confirmed by both the X-ray observations of the quiescent X-ray emission from Sgr A* (Wang et al. 2013) and the recent Event Horizon Telescope observations at 1.3 mm (Psaltis et al. 2014). The elongation direction is also consistent with the well-constrained value, $\sim 90 - 100^\circ$, inferred from the recent mm-VLBA observations (Bower et al. 2014b). While the X-ray emission traces the accretion flow in outer regions, the mm emission in innermost ones. Therefore, we may consider that the inclination angle of the accretion flow is well determined by that of the stellar disk. Adopting the value of 53° gives a RM less than 10^4 rad m^{-2} , much smaller than the observed value.

Finally, the jet model itself has a constraint on the inclination angle, which is $\theta_i \approx 55^\circ$ or 60° (for the “old” jet model, but see below for the updated one) for the power-law or the thermal distributions, respectively. Either of these two values is smaller than the “required” value of $\theta_i \gtrsim 73^\circ$. This means that, if we reasonably assume that jet is perpendicular to the accretion flow, the jet model fails to explain the observed RM.

However, with the further consideration of the 7-mm VLBA data in the spectral energy distribution analysis, the updated jet model (Markoff et al. 2007) constrains the inclination angle as $\theta_i \gtrsim 75^\circ$ and a position angle in the sky as 105° . With this large angle, we find that the updated jet model could have a RM chiefly in the foreground accretion flow comparable to the observed one. But in this case, the direction of the jet is completely inconsistent with that of the stellar disk.

Are there any other contributions to the RM in addition to the plasma within the jet and the accretion flow considered above? One possibility is from the ISM (interstellar medium). However, several studies have concluded that the ISM contribution to the RM is much less than $\sim 10^4 \text{ rad m}^{-2}$ due to the weaker magnetic field ($\lesssim 1 \text{ mG}$; e.g., Han et al. 1999; Baganoff et al. 2003;

Marrone et al. 2007). The recent discovered magnetar PSR J1745 – 2900 close to Sgr A* with a projected offset of $\sim 3'' = 0.12 \text{ pc}$ shows a $\text{RM} = (-6.696 \pm 0.005) \times 10^4 \text{ rad m}^{-2}$ (Eatough et al. 2013). The recent VLBA observations further demonstrate that PSR J1745 – 2900 shares the same scattering medium with Sgr A* (Bower et al. 2014a). Therefore, one may conclude that the ISM contribution to the RM is far below the value observed toward Sgr A* itself (Marrone et al. 2007).

Therefore, the “old” jet model may be ruled out, whereas the new one requires that the jet direction deviates significantly from being perpendicular to the accretion flow due to some unknown reasons.

5. SUMMARY

We have calculated the expected RM from the jet model of Sgr A*. We find that the contribution to the RM from the jet is estimated to be less than $7.7 \times 10^3 \text{ rad m}^{-2}$, while the observed RM is $5.6 \pm 0.7 \times 10^5 \text{ rad m}^{-2}$ (the minus sign ignored). We have then further considered the RM contribution from the sightline passage through the foreground accretion flow and find that its angle relative to our LOS needs to be larger than $\theta_i \gtrsim 73^\circ$, assuming that the jet is perpendicular to the accretion flow. But this requirement of the inclination angle is inconsistent with either, $\theta_i \approx 55^\circ - 60^\circ$, set by the “old” jet model itself (Falcke & Markoff 2000) or $\sim 53^\circ$, set by the stellar disk inclination. Therefore, the “old” jet model can firmly be rejected. The updated jet model with a highly inclined LOS, however, cannot be ruled out by the current RM observation alone. The jet direction predicted by the model appears to be inconsistent with the axis of the accretion flow. The future high precision imaging data lending more stringent constraints on the putative jet and/or the inclination and size of the accretion flow could finally break the degeneracy of the theoretical models.

We thank Sera Markoff, Heino Falcke, Geoffrey Bower for the constructive discussions and the anonymous referee for useful comments. This work was supported in part by the Natural Science Foundation of China (grants 11103061, 11133005, 11121062, and 11103059), the National Basic Research Program of China (973 Program, grant 2014CB845800), and the Strategic Priority Research Program “The Emergence of Cosmological Structures” of the Chinese Academy of Sciences (grant XDB09000000).

REFERENCES

- Aitken, D. K., Greaves, J. S., Chrysostomou, A., Jenness, T., Holland, W., Hough, J. H., Pierce-Price, D., & Richer, J. 2000, *ApJ*, 534, L173
- Asada, K., Inoue, M., Uchida, Y., et al. 2002, *PASJ*, 54, L39
- Baganoff, F. K., et al. 2003, *ApJ*, 591, 891
- Begelman, M. 2012, *MNRAS*, 420, 2912
- Blandford, R. & Begelman, M. 1999, *MNRAS*, 303, L1
- Bower, G. C., Falcke, H., Wright, M. C., & Backer, D. C. 2005, *ApJL*, 618, L29
- Bower, G. C., Deller, A., Demorest, P., et al. 2014a, *ApJL*, 780, L2
- Bower, G. C., Markoff, S., Brunthaler, A., et al. 2014b, *arXiv:1405.1456*
- Broderick, A. E., Fish, V. L., Doeleman, S. S., & Loeb, A. 2011, *ApJ*, 735, 110
- Burn, B. J. 1966, *MNRAS*, 133, 67
- Cioffi, D. F., & Jones, T. W. 1980, *AJ*, 85, 368
- Cooper, B. F. C., & Price, R. M. 1962, *Nature*, 195, 1084
- Cuadra, J., Nayakshin, S., Springel, V., & Di Matteo, T. 2006, *MNRAS*, 366, 358
- Cuadra, J., Nayakshin, S., & Martins, F. 2008, *MNRAS*, 383, 458
- De Villiers, J. P., Hawley, J. F., Krolik, J. H., & Hirose S. 2005, *ApJ*, 620, 878
- Dexter, J., Agol, E., Fragile, P. C., & McKinney, J. C. 2010, *ApJ*, 717, 1092
- Doeleman, S. S., Weintroub, J., Rogers, A. E. E., et al. 2008, *Nature*, 455, 78
- Eatough, R. P., Falcke, H., Karuppusamy, R., et al. 2013, *Nature*, 501, 391
- Falcke, H. & Markoff, S. 2000, *A&A*, 362, 113 (FM00)

- Falcke, H. & Markoff, S. 2013, *Classical and Quantum Gravity*, 30, 244003
- Genzel, R., Eisenhauer, F. & Gillessen, S. 2010, *Rev. Mod. Phys.*, 82, 4
- Gabuzda, D. C., Murray, É., & Cronin, P. 2004, *MNRAS*, 351, L89
- Ghez, A. M., Salim, S., Weinberg, N. N., et al. 2008, *ApJ*, 689, 1044
- Gillessen, S., Eisenhauer, F., Fritz, T. K. et al. 2009, *ApJL*, 707, L114
- Han, J.L., Manchester, R.N. & Qiao, G. J. 1999, *MNRAS*, 306, 371
- Hawley, J. F. & Balbus, S. A. 2002, *ApJ*, 573, 738
- Homan, D. C. 2012, *ApJL*, 747, L24
- Huang, L., Cai, M., Shen, Z.-Q., & Yuan, F. 2007, *MNRAS*, 379, 833
- Igumenshchev, I. V., Narayan, R. & Abramowicz, M. A. 2003, *ApJ*, 592, 1042
- Li, J., Ostriker, J., & Sunyaev, R. 2013, *ApJ*, 767, 105
- Macquart, J.P. et al. 2006, *ApJ*, 646, L111
- Manmoto, T., Mineshige, S., & Kusunose, M. 1997, *ApJ*, 489, 791
- Markoff, S., Bower, G. C., & Falcke, H. 2007, *MNRAS*, 379, 1519
- Markoff, S., Falcke, H., Yuan, F. & Biermann, P. 2001, *A&A*, 379, L13
- Marrone, D. P., Moran, J. M., Zhao, J.-H. & Rao, R. 2007, *ApJL*, 654, L57
- McKinney, J. C., Tchekhovskoy, A. & Blandford, R. 2012, *MNRAS*, 423, 3083
- Melia, F. 1992, *ApJ*, 387, L25
- Melia, F., Liu, S. & Coker, R. 2000, *ApJ*, 545, L117
- Meyer, L., Ghez, A.M., Schödel, R., et al. 2012, *Science*, 338, 84
- Mościbrodzka, M., Gammie, C. F., Dolence, J. C., Shiokawa, H., & Leung, P. K. 2009, *ApJ*, 706, 497
- Mościbrodzka, M., & Falcke, H. 2013, *A&A*, 559, L3
- Narayan, R., Igumenshchev, I.V., & Abramowicz, M. A. 2000, *ApJ*, 539, 798
- Narayan, R., Igumenshchev, I. V., & Abramowicz, M. A. 2003, *PASJ*, 55, L69
- Narayan, R., Yi, I., & Mahadevan, R., 1995, *Nature*, 374, 623
- Narayan, R., Sądowski, A., Penna, R. F. & Kulkarni, A. K. 2012, *MNRAS*, 426, 3241
- Narayan, R., Mahadevan, R., Grindlay, J. E., Popham, R. G., & Gammie, C. 1998, *ApJ*, 492, 554
- Paumard, T., Genzel, R., Martins, F., et al. 2006, *ApJ*, 643, 1011
- Psaltis, D., Narayan, R., Fish, V. L., et al. 2014, *arXiv:1409.5447*
- Quataert, E., & Gruzinov, A. 2000a, *ApJ*, 539, 809
- Quataert, E., & Gruzinov, A. 2000b, *ApJ*, 545, 842
- Schödel, R., Ott, T., Genzel, R., et al. 2002, *Nature*, 419, 694
- Sharma, P., Quataert, E., & Stone, J. M. 2007, *ApJ*, 671, 1696
- Shcherbakov, R. V., Penna, R. F., & McKinney, J. C. 2012, *ApJ*, 755, 133
- Stone, J.M., Pringle, J. E. & Begelman, M. 1999, *MNRAS*, 210, 1002
- Taylor, G. B. 1998, *ApJ*, 506, 637
- Taylor, G. B. 2000, *ApJ*, 533, 95
- Tchekhovskoy, A., & McKinney, J. C. 2012, *MNRAS*, 423, L55
- Tchekhovskoy, A., Narayan, R., & McKinney, J. C. 2011, *MNRAS*, 418, L79
- Udomprasert, P. S., Taylor, G. B., Pearson, T. J., & Roberts, D. H. 1997, *ApJL*, 483, L9
- Wang, Q. D., Nowak, M. A., Markoff, S. B., et al. 2013, *Science*, 341, 981
- Yuan, F., Bu, D. & Wu, M. 2012, *ApJ*, 761, 130
- Yuan, F., Markoff, S., & Falcke, H. 2002, *A&A*, 383, 854
- Yuan, F., & Narayan, R. 2014, *ARA&A*, 52, 529
- Yuan, F., Quataert, E., & Narayan, R. 2003, *ApJ*, 598, 301
- Yuan, F., Shen, Z.-Q., & Huang, L. 2006, *ApJL*, 642, L45
- Yuan, F., Wu, M., & Bu, D. 2012, *ApJ*, 761, 129
- Zavala, R. T., & Taylor, G. B. 2002, *ApJL*, 566, L9
- Zavala, R. T., & Taylor, G. B. 2003, *ApJ*, 589, 126